Computational Imaging on the Electric Grid

Supplementary Material

Mark Sheinin, Yoav Y. Schechner
Viterbi Faculty of Electrical Engineering
Technion - Israel Institute of Technology
marksheinin@gmail.com, yoav@ee.technion.ac.il

Kiriakos N. Kutulakos
Dept. of Computer Science
University of Toronto
kyros@cs.toronto.edu

Abstract

This is a supplementary document to the main manuscript [9]. Here we provide details that, due to page-space considerations, do not appear in [9]. This supplementary document provides more details about the DELIGHT database and the camera prototype (ACam) used in experiments. It also describes an intermediate refinement step that assists unmixing, as we used in the experiments. We show additional experimental examples.

1. This Supplementary, in General

We highly recommend the reader to watch the supplementary videos that appear in [10, 11]. In the text herein we provide details that do not appear in [9] due to page limits there. Specifically, we give details about the DELIGHT database, which is available in [10] and is used to compute *bulb response functions* (BRFs) for various types of bulbs common indoors and outdoors. Details about DELIGHT are available in Section 2.

In Section 3 we provide additional technical details about ACam operation, including a calibration procedure to compensate for Arduino delay. Section 4 provides additional experimental results, including a ground truth lab experiment whose results appear in Figure 1[bottom] of the main manuscript, as well as, results of semi-reflection separation mentioned without detail in [9].

Unless otherwise stated, all numbering of equations, sections, and figures herein refer to entities within this supplementary document. Whenever we refer to an object of the main manuscript [9], we say so explicitly.

2. DELIGHT Details

Databases have contributed immensely to computer vision and graphics [2, 3, 4, 6, 5, 8, 13, 15], particularly in determining subspaces of physics-based effects. Our paper provides a missing link: a database of BRFs, which dominate indoor and nocturnal outdoor lighting. As we show in the main manuscript [9], the database is very helpful for computer vision on the electric grid, particularly for recognition of grid phase and bulb type at a distance, as well as unmixing, white balancing and relighting.

Fig. 1. Bulbs and fixtures collection in DELIGHT.

The database is described in Section 3 of the main manuscript [9]. Here we give a more detailed account. Bulb BRFs were captured in three ways:
(1) BRFs were sensed using a TEMT6000 Ambient Light Sensor, in parallel to measuring the AC voltage $V(t)$ at the reference outlet. The reference outlet was selected arbitrarily. Color filters were used to measure different color channels. Each bulb folder contains between 100 and 400 identical measurements triggered by a positive-to-negative zero-crossing of the AC voltage.[1] These multiple measurements are averaged and clipped between two zero crossings to produce a noise-free BRF.
(2) Here, we used the same setup as in (1) but without any filters.
(3) We pointed our ACam, fitted with a Prosilica GT1920C

[1]The actual data capturing begins with a slight delay after the zero-crossing.

color camera, at a white sheet and captured a K-frame sequence. BRFs were produced by averaging the normalized signal $\dot{\mathbf{i}}^{\text{norm}}(\sigma)$ of many pixels on the white sheet. Table 1 details the bulbs measured, so far. Figure 1 herein shows bulbs that were used. We found that new LED bulbs show an interesting variability or BRFs across brands. Figure 2[Bottom-Left] of the main manuscript [9] shows raw bulb measurements using the photodiode. Figure 2[Bottom-Right] shows the averaged, low-noise BRFs, extracted using the multiple raw measurements.

3. ACam Technical Details

The ACam is mainly described in Section 6 of the main manuscript [9]. We implemented an ACam prototype by adapting the system described in [7]. Our adaptation adds an Arduino Due controller to synchronize the DMD shuttering to the AC grid. We feed the Arduino with a reduced version of the raw AC voltage in the reference outlet. The AC voltage is reduced so as to span the Arduino's analog input voltage range, in our design 0 to 3.3V.

For the inner-camera module, our experiments used Allied Vision Prosilica GT 1920, relying either on color or monochrome (BW) sensors.

3.1. Controller Delay Calibration

The ACam tracks zero-crossings in real time. During capture of frame $k \in K$, the Arduino repeatedly detects AC voltage zero-crossings. Once a zero-crossing is detected, the Arduino exposes sub-frame k by holding mask $\mathbf{0}$ for $[(k-1)\Delta]/K$ seconds before switching to mask $\mathbf{m}_m$ (see Figure 7 in main manuscript). However, in practice, electronic imperfections may introduce a constant delay between zero-crossing detection and switching to mask $\mathbf{m}_m$. This delay causes a slight and constant phase shift $\Delta\phi_{\text{Ard}}$ to the K-frame sequence $\mathbf{I}$. Such a constant phase shift effects tasks that rely on DELIGHT BRFs; scene BRFs may be slightly shifted, compared to database BRFs.

To compensate for this phase shift, we find $\Delta\phi_{\text{Ard}}$ by imaging a *known scene* bulb, e.g. a Sodium lamp, which is abundant in outdoor scenes. Then, $\Delta\phi_{\text{Ard}}$ is determined as the phase difference between the measured BRF and the corresponding DELIGHT BRF. This calibration is done once per camera and operating conditions; $\Delta\phi_{\text{Ard}}$ is then applied to all measured $\mathbf{I}$.

3.2. Re-syncing to AC

Due to random wiggle of the AC frequency, the ACam is locked to last-detected zero crossing. In practice, locking the camera to *every* zero-crossing is technically more involved.

Fortunately, the temporal blur effect shown in Figure 9 of the main text is cumulative. Hence, while this effect accumulates over the entire exposure time, it is practically negligible in the span of few tens of cycles. Therefore, re-syncing need not be done at every AC cycle. In our experiments, we re-synced the camera every 10 cycles. This enabled a much simpler controller implementation, while having virtually no effect of the acquired sequence.

4. More About The Experiments

4.1. Ground Truth Experiment

Figure 2 herein describes a controlled lab experiment. Five different sources illuminated the scene, each arbitrarily connected to one of the grid phases $\mathbb{P} \in \{0, 2\pi/3, 4\pi/3\}$. Each source is a known bulb from DELIGHT. The ACam integrated light during $C = 1000$ cycles. The camera gain was 0. Unmixing used DELIGHT BRFs. Videos of $\hat{\mathbf{I}}_s$ are shown in [10, 11]. Being a lab setting, there is ground truth to $\mathbf{I}_s$: it was obtained by switching off all bulbs, while turning on exclusively only source s. The comparison to ground truth is shown in Figure 2. Figure 3 shows the effect of refinement described in Eq. (18) of the main text for one of the sources shown in Figure 2.

4.2. Semi-Reflection Separation

In the main manuscript [9], Section 5.3 shows that bulb flicker can be used for separating semi-reflections passively, using two mechanisms. Section 5.3 in the main manuscript describes the second mechanism, in which a scene illuminated by *two* light sources, one fed by AC voltage and one natural, is unmixed without prior knowledge of scene BRFs.

Here we show results for the first mechanism, which is more general and can be used to unmix scenes with an arbitrary number of illumination sources. The first mechanism, however, requires knowing the sources' BRFs. This is a new principle, relative to prior methods [1, 12, 14, 16] of semi-reflection separation that had relied on motion, active flash/no-flash, polarization and defocus.

In Figure 4, both the indoor semi-reflected component and the outdoor transmitted component are under AC lighting. Indoor lighting inside the building is by sources connected to the different grid phases, yet all of them use bulb type CFL-F that appears in DELIGHT. Outdoor lighting outside this building is by sodium and fluorescent bulbs. ACam integrated $C = 1200$ cycles. The camera gain was set to 25. Figure 4 shows the three semi-reflected components.

References

[1] A. Agrawal, R. Raskar, S. K. Nayar, and Y. Li. Removing photography artifacts using gradient projection and flash-exposure sampling. In *ACM SIGGRAPH*, 24(3):828–835, 2005.

Type	Brand	Power	Name	Sensing Method
Incandescent	OSRAM	60W	Incand1	(2),(3)
Incandescent	TUNGSRAM L5 LM	100W	Incand2	(2)
Incandescent	ONOUR	100W	Incand3	(2)
Incandescent	LUXLIGHT 17/6	100W	Incand4	(2)
Incandescent	LUXLIGHT 17/6	100W	Incand5	(2)
Incandescent	HATCHI	100W	Incand6	(2)
Fluorescent 60cm	LUXLIGHT L18 W/765-Fixt. 1	18W	Fluores1	(1),(2),(3)
Fluorescent 60cm	LUXLIGHT L18 W/765-Fixt. 2	18W	Fluores1_f2	(2)
Fluorescent 60cm	LUXLIGHT L18 W/765-Fixt. 3	18W	Fluores1_f3	(2)
Fluorescent 60cm	LUXLIGHT L18 W/765	18W	Fluores2	(2)
CFL	OSRAM DULUX S	7W	CFL 2U	(2),(3)
CFL	OSRAM	11W	CFL2	(2)
CFL	ELECTRA MINI STAR 6500K	23W	CFL3	(2)
CFL	PHILIPS PL E-T	23W	CFL4	(2)
CFL	LEELITE 6500K	11W	CFL5	(2)
CFL	unknown 6500K	32W	CFL6	(2)
CFL	NEPTON Daylight 1022lm	20W	CFL7	(2)
CFL	HYUNDAI ECO T2 2700K	15W	CFL8	(2)
CFL	NEPTON Daylight 1022lm	20W	CFL9	(2)
CFL	LEELITE 6400K	11W	CFL10	(2)
CFL	PHILIPS MASTER PL-C	18W	CFL-F	(1),(2),(3)
Halogen	SYLVANIA E06D	42W	Halogen1	(2)
LED	LEELITE 3000K	6W	LED1	(2)
LED	SAYNET 6500K	3W	LED2	(2),(3)
LED	SEMICON	17W	LED3	(2)
LED	ELECTRA LED 530	12W	LED4	(2)
LED	SEMICON	18W	LED5	(2)
LED	FSL	11W	LED6	(2)
LED	EUROLUX 6000K	30W	LED7	(2)
Sodium	ORSAM VIALOX	70W	Sodium	(1),(2),(3)
Mercury	ORSAM HQL (MBF-U)	125W	Mercury	(2),(3)
Metal Halide	ORSAM HQI-T W/D PRO	250W	MH1	(2),(3)

Table 1. List of light bulbs in DELIGHT so far. All bulbs in this table were measured under the 50Hz/220V AC standard. The last column indicates the type of measurement available for each bulb, according to the method numbering in Section 2.

[2] K. J. Dana, B. Van Ginneken,S. K. Nayar and J. J. Koenderink. Reflectance and texture of real-world surfaces. *ACM TOG*, 18(1), 1–34 ,1999.

[3] M. D. Grossberg, and S. K. Nayar. What is the space of camera response functions?. In *Proc. IEEE CVPR* , 2:602–609, 2003.

[4] D. Martin, C. Fowlkes, D. Tal, and J. Malik. A database of human segmented natural images and its application to evaluating segmentation algorithms and measuring ecological statistics. In *Proc. IEEE ICCV* , 2, 416–423, 2001.

[5] S. G. Narasimhan, M. Gupta, C. Donner, R. Ramamoorthi,S. K. Nayar and H.W. Jensen. Acquiring scattering properties of participating media by dilution. In *ACM SIGGRAPH*, 1003–1012 ,2006.

[6] S. G. Narasimhan, C. Wang and S. K. Nayar. All the images of an outdoor scene. In *Proc. ECCV* , 148–162, 2002.

[7] M. O'Toole, J. Mather and K. N. Kutulakos. 3d shape and indirect appearance by structured light transport. In *Proc. IEEE CVPR* , 2014.

[8] D. Scharstein and R. Szeliski. A taxonomy and evaluation of dense two-frame stereo correspondence algorithms. In *Intren. Journal of Comp. Vision* , 47(1/2/3):7–42, 2002.

[9] M. Sheinin, Y. Y. Schechner, and K. N. Kutulakos. Computational Imaging on the Electric Grid. In *Proc. IEEE CVPR*, 2017.

[10] *Computational Imaging on the Electric Grid: Webpage*. [Online] (2017). Available at: http://webee.technion.ac.il/˜yoav/research/ACam.html

[11] *Computational Imaging on the Electric Grid: Project webpage*. [Online] (2017). Available at: http://www.dgp.toronto.edu/ACam

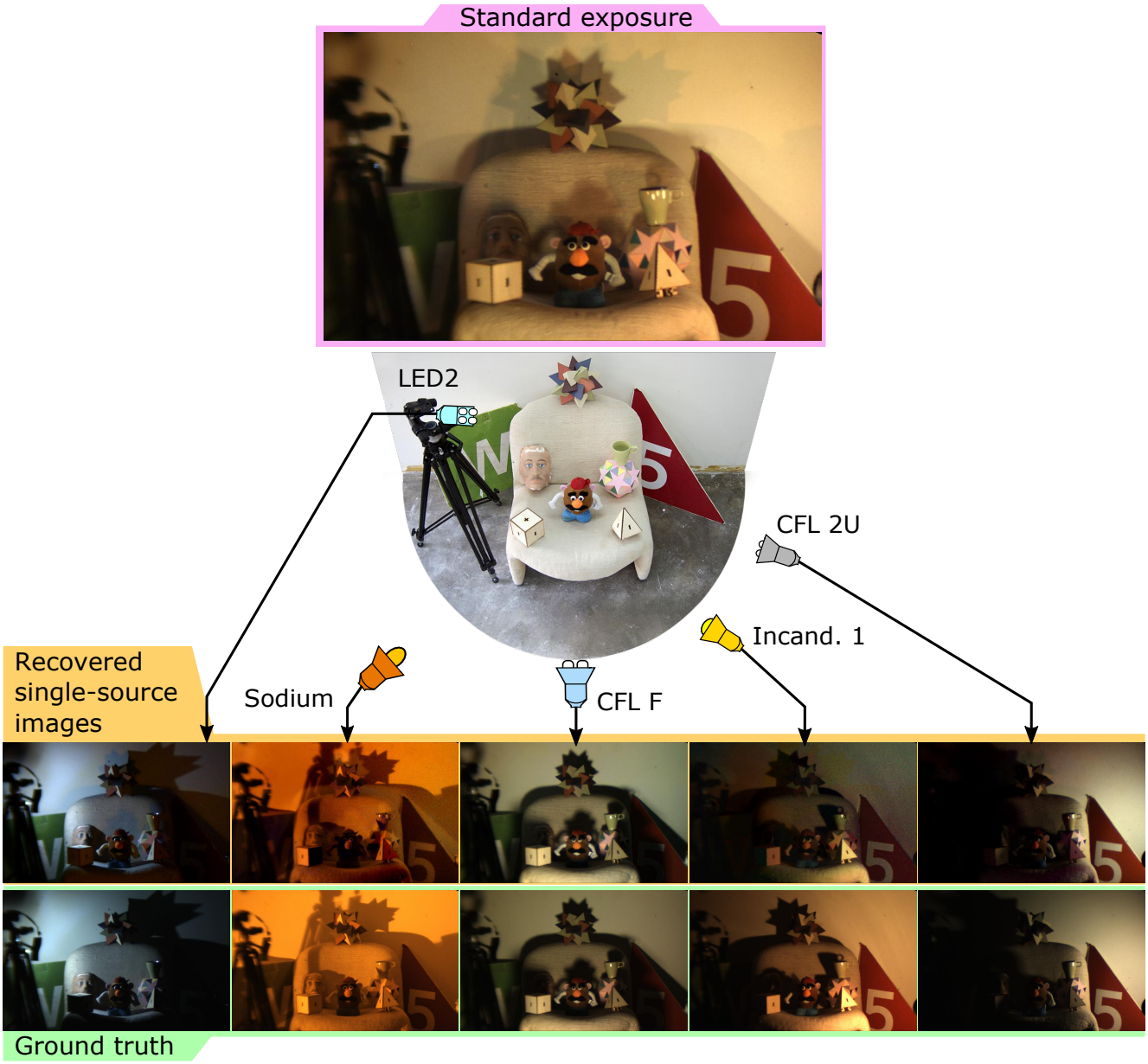

Fig. 2. Ground truth experiment. A scene illuminated by five bulbs each connected to one of three grid phases $\phi \in \mathbb{P}$ [Middle]. A standard exposure image mixes lighting components [Top]. ACam sampled the scene, creating a sequence of $K = 26$ sub-cycle samples (see video in [10, 11]). The scene was unmixed using bulb BRFs from DELIGHT [Top row]. Unmixing was consistent with ground truth [Bottom row] that was obtained by lighting the scene with each bulb individually.

[12] S. Shwartz, Y. Y. Schechner, and M. Zibulevsky. Efficient separation of convolutive image mixtures. In *Proc. Inter. Conf. on ICA and BSS*, 246–253, 2006.

[13] T. Sim, S. Baker, and M. Bsat. The CMU pose, illumination, and expression (PIE) database. In *Proc. IEEE Intern. conf. on Automatic Face and Gesture Recog.* , 46–51, 2002.

[14] S.N. Sinha,J. Kopf,M. Goesele, D. Scharstein, and R. Szeliski. Image-based rendering for scenes with reflections. In *ACM TOG*,31(4):1–10, 2006.

[15] G. Stratou, A. Ghosh, P. Debevec, and L. P. Morency. Effect of illumination on automatic expression recognition: a novel 3D relightable facial database. In *Proc. IEEE Intern. conf. on Automatic Face and Gesture Recog.* ,611–618, 2011.

[16] A. Levin, and Y. Weiss. User assisted separation of reflections from a single image using a sparsity prior. In *IEEE Trans. PAMI*, 29(9), 1647, 2011.

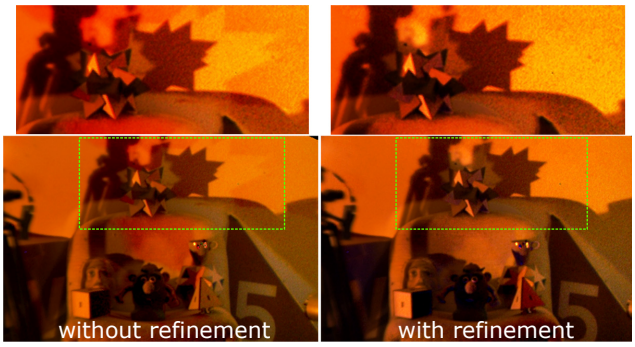

Fig. 3. Recovered single-source images of sodium bulb in Figure 2 [Bottom]. An inset is magnified and contrast-stretched at the [Top]. Minor artifacts [Left] are removed by a refinement step[Right].

Fig. 4. Semi-reflection separation for an AC-Illuminated scene experiment. An indoor scene is illuminated by CFL-F bulbs, each connected to an arbitrary AC phase $\phi \in \mathbb{P}$. The ACam is placed inside the lobby, facing outside. The indoor scene in (a) is semi-reflected by a lobby glass door. The outdoor scene the camera is facing is (b). At night, the outdoor scene is illuminated by a Sodium lamp. A standard exposure image shows a mixture of the semi-reflected and transmitted components. ACam captured a $K = 26$ sequence using $C = 1200$ and a camera gain of 25 (see video in [10, 11]). The scene was unmixed using $S = 4$ source taken from DELIGHT.